Mater. Res. Soc. Symp. Proc. Vol. 1656 © 2014 Materials Research Society
DOI: 10.1557/opl.2014.711

Quantitative Porosity Studies of Archaeological Ceramics by Petrographic Image Analysis

Chandra L. Reedy[1], Jenifer Anderson[1], Terry J. Reedy[2]

[1]Center for Historic Architecture & Design, University of Delaware, Newark, DE 19716, USA
[2]Independent Statistician, 3 Stage Road, Newark, DE, 19711, USA

ABSTRACT

Pores in archaeological ceramics can form in a number of different ways, and reflect both deliberate choices and uncontrollable factors. Characterizing porosity by digital image analysis of thin sections holds a number of advantages as well as limitations. We present the results of experiments aimed at improving this method, focusing on high-resolution scans of entire thin sections. We examine the reproducibility of pore measurements by petrographic image analysis of ceramic thin sections using laboratory-prepared specimens of clay mixed with sand of known amount and size. We outline protocols for measuring Total Optical Porosity, using the Image-Pro Premier software package. We also briefly discuss use of pore size and pore shape (aspect ratio and roundness) in characterizing archaeological ceramics. While discerning reasons for observed amounts, sizes, and shapes of pores is an extremely complex problem, the quantitative analysis of ceramic porosity is one tool for characterizing a ware and comparing a product to others. The methods outlined here are applied to a case study comparing historic bricks from the Read House in New Castle, Delaware; the porosity studies indicate that different construction campaigns used bricks from different sources.

INTRODUCTION

Porosity has long been recognized as an important feature to characterize in any study of ceramics [1]. Porosity in ceramic materials results from choices in raw materials, clay processing and object fabrication methods, drying and firing regimes, and use, burial, or deterioration factors [2-4]. For example, during clay processing and vessel fabrication, air bubbles can become trapped. Shrinkage during drying and firing can enlarge those pores. Long linear pores with parallel alignment, often wavy with tapering ends, can appear as a result of shrinkage of the clay as excess water is released during firing; this alignment may also emphasize patterns of pressure placed during fabrication. At higher firing temperatures these linear pores may be less interconnected than at lower firing temperatures [5]. As carbonates dissociate and organics burn out or char during firing, additional porosity can be created. If firing temperatures are high enough, porosity can decline if vitrification occurs [1, 6]. Temper additives such as sand or grog can keep porosity higher, as clay tends to shrink away from those particles during drying and firing, creating additional porosity. Round secondary pores can be produced by trapped gases as the clay matrix and silica minerals begin to melt, off-gas, and vitrify [7]. If temperatures become too high, the round pores can become bloated and expand in number, indicating overfiring.

Some ceramics are deliberately designed to be porous for certain functions, while others are designed with low porosity. Vessels intended for cooking need to be porous enough to expand and contract over a fire without cracking, and storage ceramics intended to keep contents

cool need a pore structure that allows evaporation; during use these pores can become enhanced. Another complication is that porosity changes can occur due to burial of a ceramic, with microcracking or dissolution from groundwater, so what is being measured may not always reflect the original material. Porosity variation within a ware, or even within areas of a single vessel, is likely to be higher for traditional ceramics compared with modern industrial products.

With so many factors affecting ceramic porosity, cultural interpretation of observed pore systems is a complex problem. Nonetheless, quantitative analysis of ceramic porosity is one tool for characterizing a ware and comparing a product to others [8]. But, with so many potential causes of porosity, relying on a bulk porosity analysis would not be as informative as being able to examine the variety in size, shape, and distribution of the pores. Being able to quantify and better understand pore characteristics are important because porosity is a direct reflection of the choices that people make in selecting and processing their materials and in fabricating and firing their ceramic products.

Archaeologists have quantitatively characterized porosity in ceramics (shape, size, number, and volume percentage) for decades [1]. A primary method has been point counting of thin sections under a transmitted light microscope. This involves superimposing a grid over the thin section and counting or measuring what is under each grid intersection point (usually with 300-400 points counted per thin section). An eyepiece micrometer is used to measure each pore. In addition to thin section analysis, traditional techniques for measuring volume porosity of ceramic materials include liquid immersion, water absorption, liquid nitrogen, or mercury intrusion porosimetry. Most of these methods are limited to measuring open pores connected to the surface and cannot access closed pores sealed off from the surface. This can sometimes lead to inaccurate or incomplete results [8, 9]; and too much sample material may be required.

Digital image analysis (DIA) of thin sections has more recently been used to quantify porosity in ceramic materials. Utilizing thin sections for this task is crucial because these can also be used for qualitative mineral identification, quantitative analysis of non-plastics, and the study of structural aspects that relate to fabrication and decorative choices. With archaeological ceramics we may not want to sacrifice the amount of sample material often required for performing tests found in ISO or ASTM standards for assessing porosity, so the relatively small sample size needed for thin sections, and the usefulness of those thin sections for addressing so many other research questions, are important considerations [10]. While some techniques for porosity measurement focus on impregnation of the material with a liquid or gaseous substance and quantify the volume of open pore spaces, DIA is a direct observation method that measures both open and closed pores [8] although it cannot distinguish between the two pore types [11]. Image analysis of petrographic thin sections has been demonstrated to provide comparable results to optical point counting and micrometer measurements, but is much faster, allowing for inclusion of a larger number of areas and specimens in quantitative work [12].

Thin section DIA focuses on measuring macropores, although the definition of these versus micropores varies considerably. In IUPAC terminology, macropores are wider than 0.05 μm; mesopores have diameters between 0.05 – 0.002 μm; and micropores are <0.002 μm diameter [13]. The limit of resolution of pores in thin sections varies depending upon the image capture system used. According to some researchers [14], pores of diameter <8 μm are not measurable with optical microscopy. Some petrographers define the boundary between macropores and micropores as a pore area of 500 μm^2, which they say translates to a pore length of about 20 μm, and close to the resolution of optical microscopy [15]. Others define microporosity as including any pores not easily detected in thin section images, and consider

these to be pore diameter of <30 μm [16]. Some researchers [9] define macropores as those about 62.5 μm, the size of fine sand [17], even with an image acquisition resolution that would allow detecting smaller pores.

Macroporosity has been found sufficient for quantifying total porosity, size, and shape of pores for most soils and ceramic materials, although this of course depends upon the research questions. Sedimentary petrographers [18] use DIA of thin sections made from undisturbed soil samples to measure pores, defining macropores as >50 μm. With our image acquisition system for scanning whole thin sections, described below, the limit of resolution we work with is generally 7 μm in length (feret diameter), with smaller pores measurable if higher scanning resolutions are used (down to about 1 μm). We are also currently experimenting with use of ultra-thin sections (15 μm thickness) for measuring smaller pores.

If adding measurements of micropores is important, and enough sample can be sacrificed, mercury porosimetry can be added. DIA of scanning electron microscope-generated images can also provide microporosity data, although some questions have been raised about their reliability for porosity studies due to variations in parameters (magnification, voltage, working distance, and detector type) leading to variable results [19], so some additional experimental work is probably also called for with these types of images; and the overall area size being examined is also an important consideration if one hopes to characterize porosity of the material as a whole.

We have been exploring ways of improving the measurement of macroporosity to characterize ceramics through DIA of thin sections. Here we first test the ease and reproducibility of DIA of pores in ceramic thin sections using 96 laboratory-prepared specimens of known recipes. We found that high-resolution scans of entire thin sections are preferable to analysis of many fields of view under the microscope. We outline our preferred protocols for measuring Total Optical Porosity using the Image-Pro Premier software package. We present data for replicate analyses of individual thin sections and for multiple specimens separately made from the same batch of raw materials. We also analyze the effect of varying amount and size of sand additives on amount of porosity after firing the experimental specimens. We conclude with a discussion of the application of this protocol to archaeological ceramics and of additional size and shape parameters that can be used to help characterize ceramic pore systems.

THIN SECTION POROSITY STUDIES

Ceramic thin sections are slices of a three-dimensional network of pores, some interconnected and others isolated. Some researchers have reported a consistent underestimation of porosity in thin sections compared with three-dimensional analysis of larger core samples [20], attributed to the presence of complex pore geometries in some specimens and to the inability to view and measure the smaller micropores; and, image analysis procedures that involve conversion to binary images may also result in the loss of some small pores [21]. However, it has been demonstrated that porosity and pore size distributions of a 3D block can be adequately predicted using 2D images [22, 23]. DIA has also been shown to be a reliable method for characterizing porosity, in agreement with results from techniques using 3D images [11]. Because thin sections are relatively low cost, easily accessible, useful for a variety of other analyses [9], and because improvements continue to be made in image analysis programs, much research has gone into DIA of thin sections.

Since sands and sandstones have similarities to ceramic materials, work on DIA performed by sedimentary geologists is relevant to ceramic studies. J. Layman [12] compared

DIA of thin sections (using Image-Pro Plus software) to other methods traditionally used by sedimentary geologists to analyze porosity. Working with carbonate rocks and averaging five fields of view for each thin section, he found it to be a reasonable substitute for determining porosity by other petrographic methods such as point-counting of thin sections; and found that pore size obtained by this method for macropores was a useful substitute for mercury porosimetry. Other sedimentary petrographers expanded the number of fields of view analyzed to ensure coverage of the entire thin section, up to 20-30 [20]. Below, we show how consistent results can be obtained by using one high-resolution scan of the entire thin section.

In the past, most ceramic thin sections were prepared using a clear epoxy resin as the mounting medium. This presents problems, since in plane polarized light the pores are difficult to differentiate from clear, low-relief quartz that is ubiquitous in most ceramic materials; and as the epoxy turns dark in crossed polarized light the empty pores are then difficult to discern from clay and quartz or other minerals in extinction position. Some ceramic petrographers tried to get around this problem by obtaining an image in both plane polarized and cross polarized light, subtracting the second image from the first, then calculating a new gray level for each pixel corresponding to the difference in value of the two images [24]. A faster and less complex approach is to impregnate the thin section with a dyed resin, so that the pores easily stand out in plane polarized light [25].

Perhaps the most useful measure for characterizing pores using image analysis is Total Optical Porosity (TOP), the ratio of the sum of all pore areas to the area of the entire image (area percentage of pores) [26] (Figure 1). Sedimentary petrographers have found other pore parameters useful as well; an advantage of DIA is that it provides simultaneous measurement of as many different parameters as one selects. In our experiments for developing a fast and reliable protocol for characterizing pores in ceramic thin sections, we focused on Total Optical Porosity.

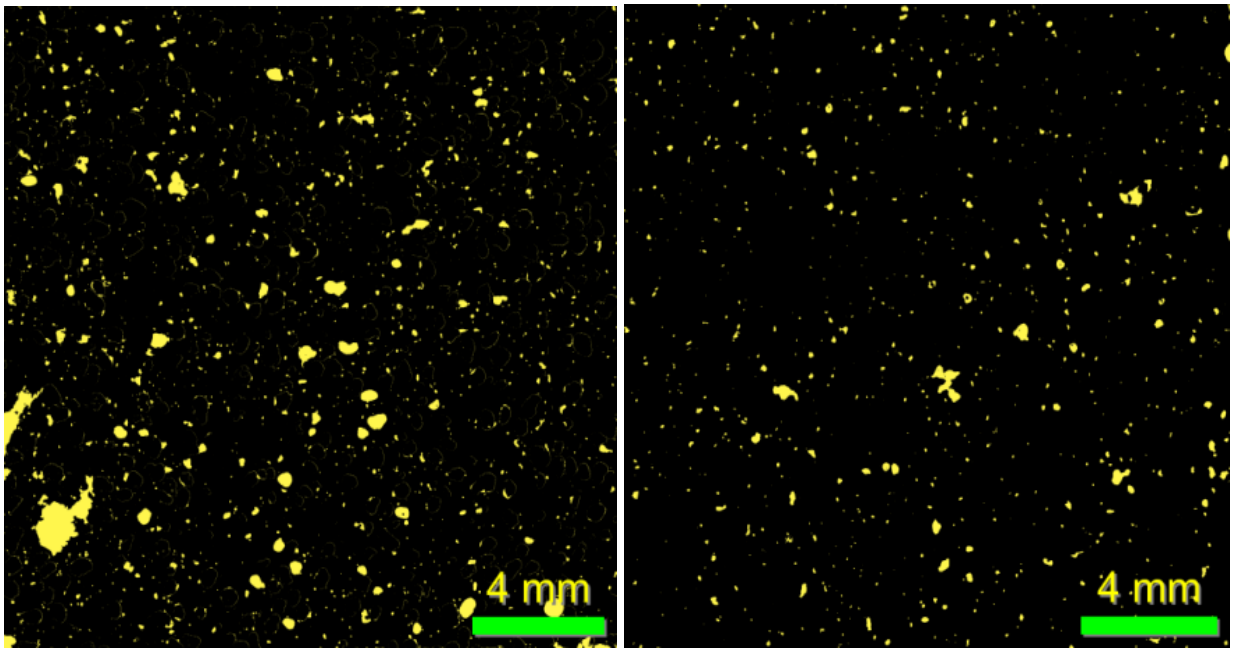

Figure 1. Pores (light areas) of two specimens, one with 4.6% Total Optical Porosity (left) and another with 2.0% Total Optical Porosity (right).

EXPERIMENTAL PROCEDURES

Experimental Units

To test image analysis protocols, we prepared a set of specimens comprised of clay and a quartz-rich sand additive. Two types of clay were used, a red earthenware that fires to a deep orange red (Earthen Red from Clay-King) and a gray earthenware that fires to a white color (White Earthenware from Clay-King), to give two very different visual appearances for the image analysis work. We picked three size ranges of sand (from Mile Hi Ceramics): coarse (16 mesh), medium (30 mesh), and fine (70 mesh). Each was then added to the clays in three different proportions: 10, 25, and 40% by volume. After kneading well, each clay-sand mixture was rolled out to an even thickness and specimens of a standard size were cut out with a cookie cutter-like mould. We deliberately chose a preparation method that would mimic how traditional potters might mix temper into a clay so that the resulting level of homogeneity would be similar to what might be encountered with ancient ceramics. Specimens were first dried in air indoors for a week, then in an oven at 150°C for another week. They were then fired with gradual increase in temperature over the course of a day, to the temperature recommended for the clays (900 - 1000ºC). This careful drying and firing regime was intended to minimize cracking or loss of grains during firing, to keep macroporosity to a minimum.

For each sand percentage, size, and clay combination, five replicate specimens were made for thin sections, for a total of 90 specimens. Another six contained clay with no sand additive (three replicates of each clay). A thin section was prepared for each of the 96 specimens.

We also investigated how much information DIA can provide on whole samples examined under a stereomicroscope, without the extra work of preparing thin sections. An advantage would be that the time and expense of thin-section cutting, mounting, and grinding would be eliminated if sherds could be characterized directly. For this research, additional replicate specimens were prepared and cut using a diamond-edge saw to obtain a fresh surface. This possibility was considered because sherds themselves, especially fresh edges or cleaned surfaces, have been used to obtain some quantitative data supplementing thin-section microscopy [27]. If DIA could be used to quantify porosity, this would allow data to be collected on even larger numbers of sherds. However, while sand grains were readily visible and with some effort could be used for image analysis, the pores in the whole specimens were difficult to see even with various processing methods. An additional problem is that only those pores open to the surface can be quantified by this method. Thus we chose to focus on thin sections.

The technique of impregnating ceramics with a dyed epoxy in thin-section preparation for DIA has been used by a number of researchers. For example, historic brick samples were mounted in a blue-dyed epoxy resin for a hue-saturation-intensity segmentation procedure (using Image-Pro Plus software) to separate the blue pores from other components of the thin sections [10]. The goal was to characterize macropores, focusing on pores at or above an area of 400 μm^2. Pottery specimens have also been prepared as blue epoxy-resin-impregnated thin sections to quantify porosity [28]; in this case a plug-in for a freeware image analysis program (Scion Image) was employed to automatically recognize the blue hues representing porosity and calculate a percentage pore abundance of the thin section. Results were contrasted with those for optical point counting and found to be comparable, but required much less time that the older method. We used a blue-dyed epoxy resin to impregnate and mount all thin section specimens.

We experimented with applying measurement protocols to multiple fields of view of a thin section under a transmitted light microscope, and then obtaining an average. However, we found this to be problematic. It is time consuming, and if there are some large pores, each field of view may be quite unrepresentative of the material as a whole, meaning that many fields of view will then have to be measured in order to be representative. An additional problem is that pores touching a border have to be discounted from any measurements other than area percentage, since they are at least partially cut off from view, so cannot be measured accurately. This reduces the number of pores available for many analyses, and affects the statistics.

Some image analysis packages have a tiling capability – so images can be taken of multiple fields of view with overlap, and then tiled and stitched together to make a single large image for analysis. Then only the grains on the border of that one large image need to be eliminated from measurements. The Image-Pro Premier software we use allows live tiling, where one can move through adjacent areas of a thin section under the microscope and a larger image is automatically tiled and stitched together. However, this too takes time and care, and creates a very large image file, so also is not ideal. As a result, we continued to search for an alternative method for processing large numbers of samples more efficiently, leading to our decision to use entire scanned thin sections for image analysis.

Images Produced in a High-Resolution Film Scanner

The solution of scanning an entire thin section has been tried by several researchers studying archaeological ceramics, historic mortars, sands, stone, and other materials [29, 30, 31]. A single image can then be used for DIA. This procedure makes quantitative analysis practical for a larger number of thin sections, and gives results that apply to the entire thin section rather than to small fields of view. One method is to use a flat-bed scanner to take high-resolution scans [9, 32-35]. For example, a flatbed scanning system was used to study macroporosity (defined as pores larger than 62.5 μm) in archaeological and historical mortars [9]. An advantage that was noted was the ability to obtain an image of the entire thin section with homogeneous illumination, something that can be difficult to achieve with multiple microscope fields of view. Color images were then converted to binary ones for analysis by ImageJ software. Flat-bed scanners have also been used to conduct DIA of pores in a variety of cementitious materials. In one case a high-resolution flat-bed scanner (3175 x 8000 dpi) was used for analysis of binary images (with pores white against a black background) for quantitative characterization of pores [36]; it was shown how much better these images were for DIA than images taken with a typical office flat-bed scanner (4800 x 4800 dpi maximum optical resolution capability).

Rather than a flat-bed scanner, thin-section scanning in a film scanner (at a resolution of 9.4 μm/pixel, incorporating polarizing filters, was successfully used in the study of texture of granitoid rocks [37]. After trying out several systems, we also chose to pursue the use of a film scanner. For this work we used a low-cost Plustek OpticFilm 7600i film scanner with maximum optical resolution of 7200 x 7200 dpi. However, scanning at maximum resolution creates very large file sizes, which can take longer for the image analysis processing, and for most image analysis work (especially on coarser ceramics) scanning at a lower optical resolution will usually suffice. A 10-mm scale bar scanned under identical conditions was used to spatially calibrate the system. If there are any glaze layers to be excluded from measurements, or areas off the edge of the thin section (showing just the epoxy) in the image, these can be excluded from measurements either by cropping the image or by using a Region of Interest mask during analysis.

Image Analysis Protocols

After experimenting with a variety of DIA software programs, we chose Image-Pro Premier software distributed by Media Cybernetics. It is intuitive and easy to use, while incorporating a wide range of operations pertinent to ceramic thin section analyses. Whichever program is used, issues that need to be considered include calibration of the image capture setup so that measurements are in a specific unit rather than in number of pixels counted, image quality (most analyses require uncompressed file formats, such as TIFF, and images must be in excellent focus), and statistical validity of the sample size for the material under analysis [25].

A major strength of the Image-Pro Premier package is its Smart Segmentation protocol. This allows one to more effectively define the reference areas for background and objects of interest in an image; the reference areas are then used to create segmentation masks to count and measure objects of interest. Smart Segmentation allows one to include a wide variety of channels for segmentation including monochrome intensity level, RGB, YIQ, and HIS color spaces and morphological filters, and to automatically correct for uneven background. It then classifies every pixel by distance to the closest reference area, using distance in multidimensional space where every segmentation channel is a dimension. Pores are highlighted by clicking on a selection of them as reference points, ensuring that the full range of colors and intensities are marked. Background is set by clicking on clay and sand (or other temper components). If the material has very small pores, zooming in for marking reference points is helpful, to ensure that the reference marks cover only the pores and do not spill over into background, and vice-versa.

For our experimental specimens, the best segmentation was achieved by RGB color channels, although other parameters were important for other archaeological ceramic products. The "fill holes" option was selected, so that if any pixels within a pore are missed in the selection of reference color ranges, they will be filled in. The parameters of the background and object areas are then analyzed, and a segmentation recipe is created which includes the transformations with maximum degree of difference between the objects and background. Multiple images can be used to construct the recipe, to ensure that the full range of variation is captured. The recipe can be saved to be applied to other similar images in a project, eliminating the need to manually mark reference areas for particles, pores, and background for many thin sections. This procedure generally works well, is fast, and is reproducible. However, when the clay is gray or white, it can sometimes have a blue tint where thin that makes it more difficult to distinguish from the blue of the pores; in this case, prior to segmentation the image can be adjusted to create more contrast between the matrix and the pores. We find that lowering the brightness and increasing the contrast makes the segmentation easier in this case.

We also found success with two alternative protocols using a different version of Image-Pro (Image-Pro Plus, also by Media Cybernetics) [38]. However, these protocols require more manual steps in image adjustment and application of filters than does the Smart Segmentation process. Whichever approach is followed, the resulting segmented areas can be carefully examined prior to going forward with measurements, to ensure that the pores have been correctly marked. Sometimes this is best done by viewing the original image side-by-side with the segmented image. Once a segmentation protocol is found to work well for the images within a research project, this process can move forward quickly.

Once the pores are correctly highlighted (segmented) (see Figure 1), any desired measurements can be performed simultaneously. The analysis can be further refined by using the classification options in Image-Pro, to identify whether or not there are clear categories of pore

diameters or shapes, and the relative abundance of each; it may then be useful to quantify these categories separately. Or, the highlighted pores can be displayed in a new image where they are sorted (Figure 2) according to length, area, aspect ratio, roundness, etc. to get a sense of the range and to inform data collection and analysis strategies. Data for each individual pore, as well as summary statistics, can be saved into a file for statistical analysis.

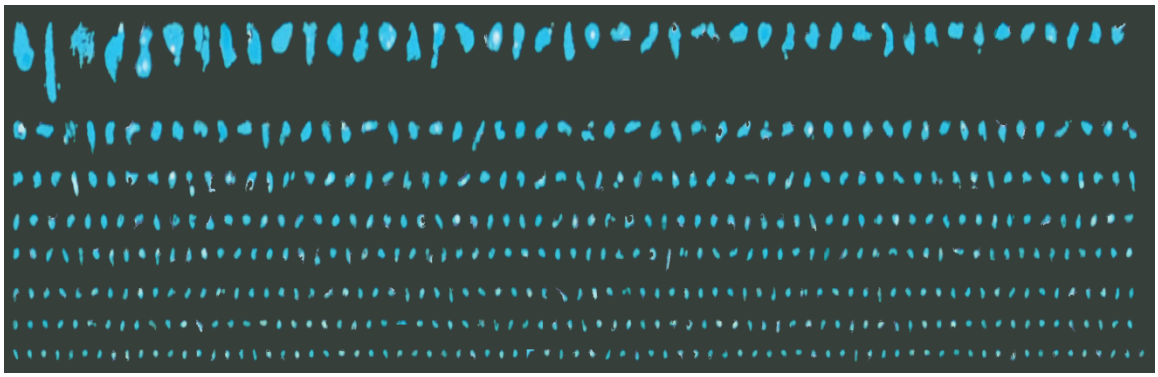

Figure 2. Here pores are sorted by size (length/ferret diameter).This type of image is useful for examining the range (here we see that most pores are very small), for deciding on cut-off points for certain measurements, and for making decisions about data collection and analysis strategies.

Once the saved segmentation recipe is correctly identifying pores, and the measurement choices have been selected, macros and batch processing can automate the procedure of opening up an image file, segmenting and measuring pores, and saving data to a file, so many scanned thin sections can be analyzed rather quickly. Data on individual pores and/or summary data can be statistically analyzed and combined with data on various particles, each segmented and analyzed with their own saved segmentation recipes and measurement parameters.

RESULTS AND DISCUSSION

We first analyzed the scanned thin sections by selecting reference points for pores and background individually for each image, choosing about 20 reference points total and trying to select the full range of colors for each component. It is possible to include multiple phases in the same analysis, by marking separate reference points for pores, sand grains, and clay background, for instance. But, given the variation in appearance within each, we found that it was easier to focus on one component at a time. Since different measurement parameters are also often selected and saved for each phase, this procedure seems more efficient.

However, it is very tedious to mark each thin-section image separately. We moved to the option in the Smart Segmentation procedure to save a recipe (parameters that give the maximum difference between the pores and the background), to reuse on other images. Not having to spend time marking each and every image allowed us to focus instead on spending more time being very careful on one representative image (or set of images), selecting 50-60 reference points. While some types of materials would not need this high number of reference points for successful segmentation, with ancient ceramics there is often much subtle variation, and this approach proved to more completely segment the full range of pore structures within the matrix. While the recipe derived from the red clay worked remarkably well for the white clay, we found that constructing a second recipe by separately marking reference points for the white clay

specimens worked better. Once the recipes were developed and saved, analysis of the remaining images proceeded quickly, by simply opening up the image and applying the recipe. For this project we did, however, carefully examine each segmented image to ensure that the recipe worked well to identify the pores without incorrectly marking any background areas as pore.

Table 1 gives the results for this analysis by carefully-constructed recipe for each of the 96 thin sections. The five numbers for each clay type and added sand size/percentage combination (three numbers for clays with no added sand) represent separate objects, each made from the same batch of clay/sand mixture. These are analogous to sherds from separate vessels made from the same batch of clay plus sand temper additive, and illustrate the variation one might expect in multiple ceramic objects made from the same clay-temper batch.

Table 1. Total Optical Porosity (Area %)

Added Sand	Red Clay	White Clay	Added Sand	Red Clay	White Clay
None	0.6	0.0	Coarse, 25%	2.2	2.9
	0.4	0.1		3.2	1.5
	0.5	0.0		2.1	1.5
Fine, 10%	1.9	1.7		2.4	1.4
	2.0	1.5		2.2	1.9
	2.4	1.6	Fine, 40%	2.7	2.2
	2.1	1.6		3.1	4.4
	2.2	1.7		3.4	1.5
Medium,10%	2.2	1.2		2.9	3.9
	3.5	1.8		2.1	2.2
	2.5	2.5	Medium,	2.9	4.4
	2.2	1.3	40%	2.5	1.6
	2.4	1.7		3.2	2.5
Coarse, 10%	2.8	1.4		3.4	1.4
	3.5	1.8		3.4	0.8
	1.5	1.3		2.4	1.9
	2.9	1.5	Coarse, 40%	2.9	4.0
	2.8	1.9		2.6	2.5
Fine, 25%	4.1	2.3		6.6	1.3
	2.8	1.1		1.9	2.1
	2.2	1.5			
	2.8	1.4			
	2.6	1.7			
Medium,	4.6	1.9			
25%	3.1	2.0			
	3.8	1.5			
	3.0	2.0			
	4.0	1.4			

Replicate specimens sampled from each batch; TOP determined on an entire scanned thin section (optical resolution 7µm/pixel). Using Smart Segmentation (Image-Pro Premier) saved recipe for each clay type, 50-60 reference points. Fine = 70 mesh; medium = 30 mesh; coarse = 16 mesh.

Table 2 shows a selected group of images analyzed by individual reference marking of 10 points each for pores and background, repeating the procedure three times for each thin section. Analyses were in random order so that a different set of reference points would get selected each time. This table shows that reproducibility of segmentation is good, with about 0.1% standard deviation for the three analyses of each image. Results for the two measurement approaches are highly correlated (Pearson Correlation Coefficient .91). However, overall pore percentages for individually measuring are somewhat lower than for applying the saved recipe (Figure 3).

Table 2. Replication with 20 Reference Points, Total Optical Porosity (Area %)

Sand %	**Red**	**Clay**		Mean	σ	**White**	**Clay**		Mean	σ
Fine, 10	1.9	1.4	1.6	1.6	0.3	1.5	1.3	1.2	1.3	0.2
Medium,10	1.9	2.3	2.0	2.1	0.2	1.0	1.0	1.0	1.0	0.0
Coarse, 10	2.0	1.9	2.0	2.0	0.1	1.2	1.1	1.1	1.1	0.1
Fine, 25	4.1	3.9	4.1	4.0	0.1	1.9	1.8	2.0	1.9	0.1
Medium, 25	3.9	4.1	4.0	4.0	0.1	1.8	1.8	2.0	1.9	0.1
Coarse, 25	1.6	1.7	1.6	1.6	0.1	2.6	2.5	2.4	2.5	0.1
Fine, 40	1.3	1.3	1.4	1.3	0.1	2.0	2.1	1.9	2.0	0.1
Medium, 40	1.7	1.7	1.7	1.7	0.0	3.5	3.6	3.8	3.6	0.2
Coarse 40	1.4	1.3	1.2	1.3	0.1	1.7	1.7	1.7	1.7	0.0

Process repeated three times for each scanned thin section.

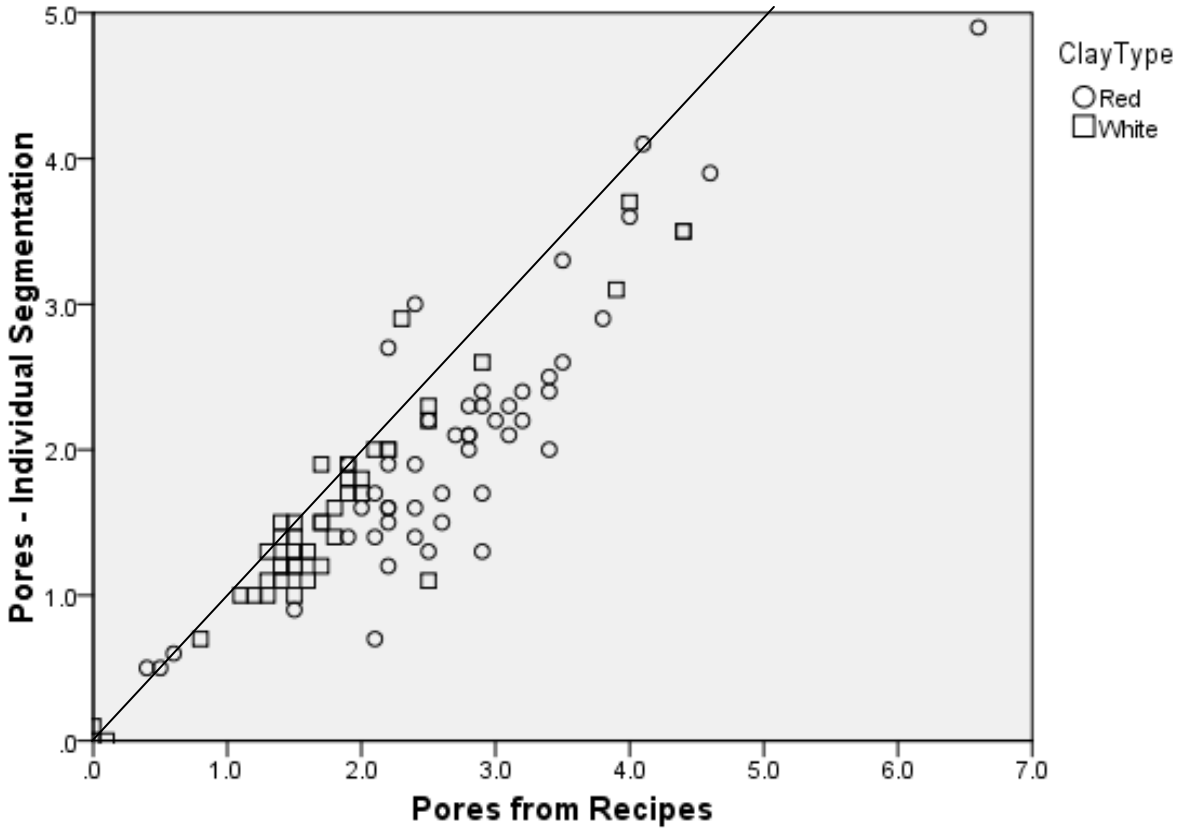

F**igure 3.** Individually-segmenting images versus applying a saved recipe are strongly correlated, but individual results are lower implying that some pores get missed.

To examine this comparison more closely, we computed a new variable, Pore Difference, as % pores identified via recipe minus % pores identified via individual measurement. This showed that most of the percentages derived from the recipe are higher, with only four cases where the individually-measured thin sections had significantly higher results. The difference between the two methods is significant, with a mean difference of 0.45% (significantly different than the 0.1% difference between individual measurements). So the approach of selecting about 10-20 new reference points on each thin section produces relatively consistent results, but gives somewhat lower percentages than obtained by using one carefully constructed (50-60 reference points) segmentation recipe in a standard way on all samples of that clay color. Examination of the images with all identified pores highlighted shows that this is not due to over fitting (marking some non-pore areas as pores), but does in fact produce a more accurately segmented image, with more of the smaller and thinner pore areas that tend to have a greenish-blue tinge being correctly identified as pores.

Why are 25-30 each pore and background points better than 10 of each? The bluish pore points form a cluster in three-dimensional space. Four points will define a tetrahedron that will exclude many pore points. As more points are added, those outside the existing bounding polyhedron will expand it. After several pore and background points have been chosen, the Image-Pro Premier software we use makes it possible to see and monitor which pore points will not be included (by using a semi-transparent mask for the pore segmentation step-by-step as it occurs) so that one may add new boundary points one at a time on a stepwise basis. A selection of 25-30 points seems to be enough to include any pores encountered, whereas 10 are not.

Some materials that are more uniform and with clearly distinct phases may require only a few points for successful segmentation. But, with the range of variation present in ancient and historic ceramic samples, the 25-30 points seem to be required consistently. For both the red and white clay specimens in this study, we did not set out to choose 25-30 points, but chose just the right number to ensure that pore areas were fully selected but no background areas incorrectly marked as pore. With the brick shown in Figure 6, where an existing recipe did not work so a new one had to be constructed, again 25 points each for pores and background produced the best result. In that case, with a brownish clay and a different blue epoxy, a different mix of RGB, HSI, and morphological characteristics formed the recipe. The ability to save the segmentation recipe and reuse it on similar images makes this careful and more time-consuming procedure more practical than it would be if we had to separately segment each and every image in a research project.

To examine the relationship between porosity and clay type, sand size, and sand amount, we did an analysis of variance (ANOVA), using the data derived from segmentation recipes. All three factors initially appeared to have a significant effect on Total Optical Porosity. However, sand size and amount might only appear to have an effect because those with no added sand have almost no porosity. Hence we redid the ANOVA with data removed for the clay with no added sand. This showed that clay type continued to be significant, but once at least 10% sand was added to the clay the sand size and amount were not significant determiners of porosity (Figure 4). This plot also clearly shows that the means for the red clay specimens are definitely higher than the means for the white clay specimens.

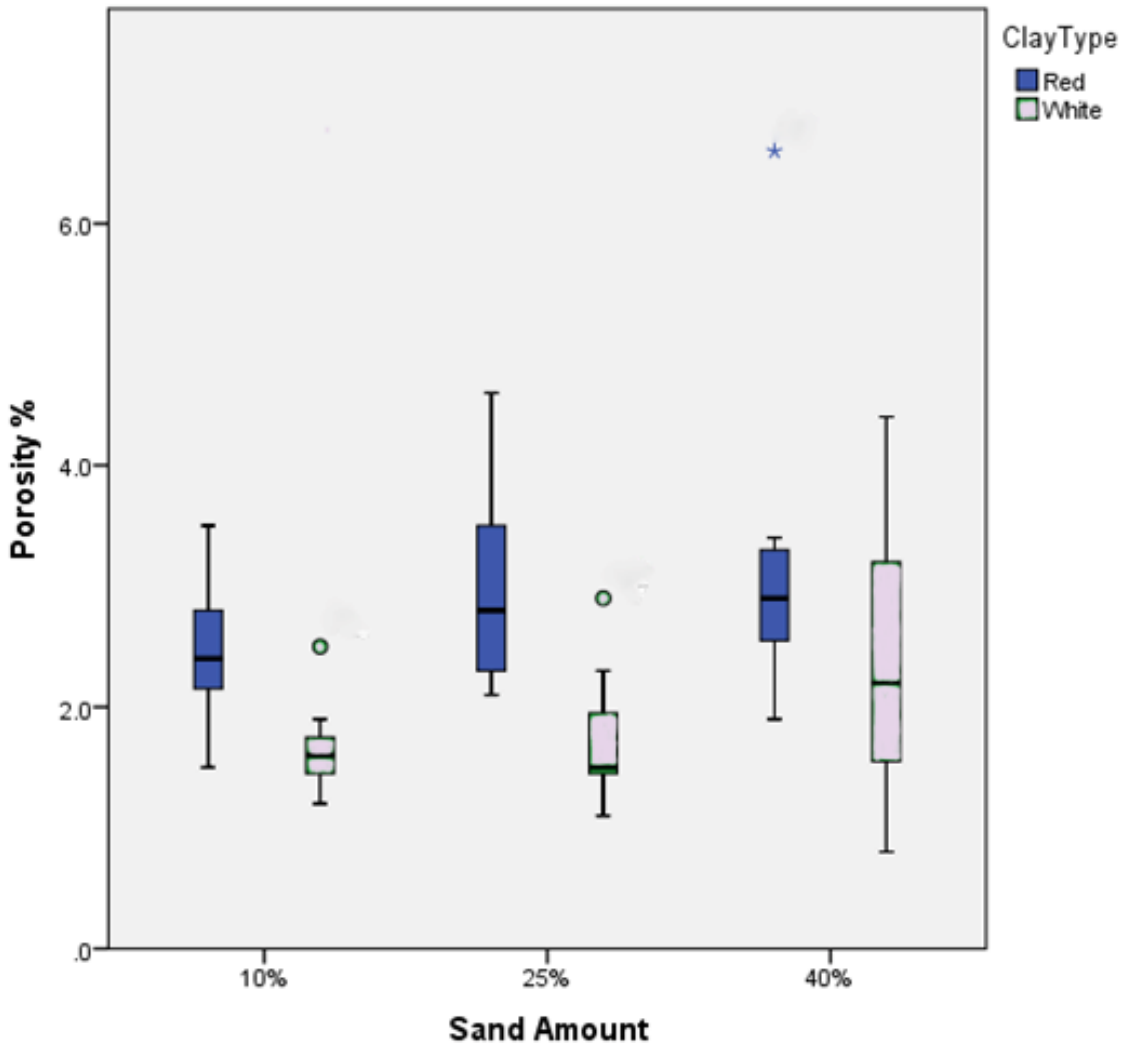

Figure 4. Box plot showing the relationship between sand amount and porosity percentage; the means for red clay specimens are higher than those for the white clay specimens, but once at least 10% sand is added, the amount has no significant effect on porosity. Brackets mark the upper and lower ranges, shaded areas the interquartile range occupied by 50% of the numbers. Outliers are separately marked.

For comparison, we analyzed a subset of thin sections using images taken at the microscope, with five fields of view in plane polarized light under 50x magnification. Since we were measuring only Total Optical Porosity, and not size and shape parameters, pores touching borders did not have to be excluded. Results of the microscope views were problematic, because there was often much variation from one field of view to another. If one or more large pores happen to be in the field of view, the area percentage is quite high; if the field of view happens to be in an area with few or only very small pores, the percentage is quite low. Since ancient ceramic materials tend not be uniform, this may always be the case. To achieve a representative

number, one would likely have to follow procedures recommended for sedimentary materials [12, 20], including as many as 20-30 images to be averaged, and possibly using an even lower power objective (to give 25x magnification). While using a saved segmentation recipe on these images could speed up analysis, it would still be time consuming to systematically mark out 20-30 fields of view, capture the digital images, and analyze them all. Using an entire scanned thin section instead makes characterizing a large number of thin sections more practical.

We have even found that one recipe can work well for multiple research projects, if the ceramic phases are similar in appearance. For example, the image in Figure 5 is a porous historic brick thin section. The pore network includes many long, stringy, narrow pores which cut across, and are embedded in, or are closely adjacent to sand grains or charred organic materials. As a result, even by zooming in closely it was often difficult to mark reference points on either pores or background without accidently touching onto the other. We decided to try the recipe already constructed for the red clay in our experimental study. Fortunately, it worked quite well at correctly highlighting the pore network.

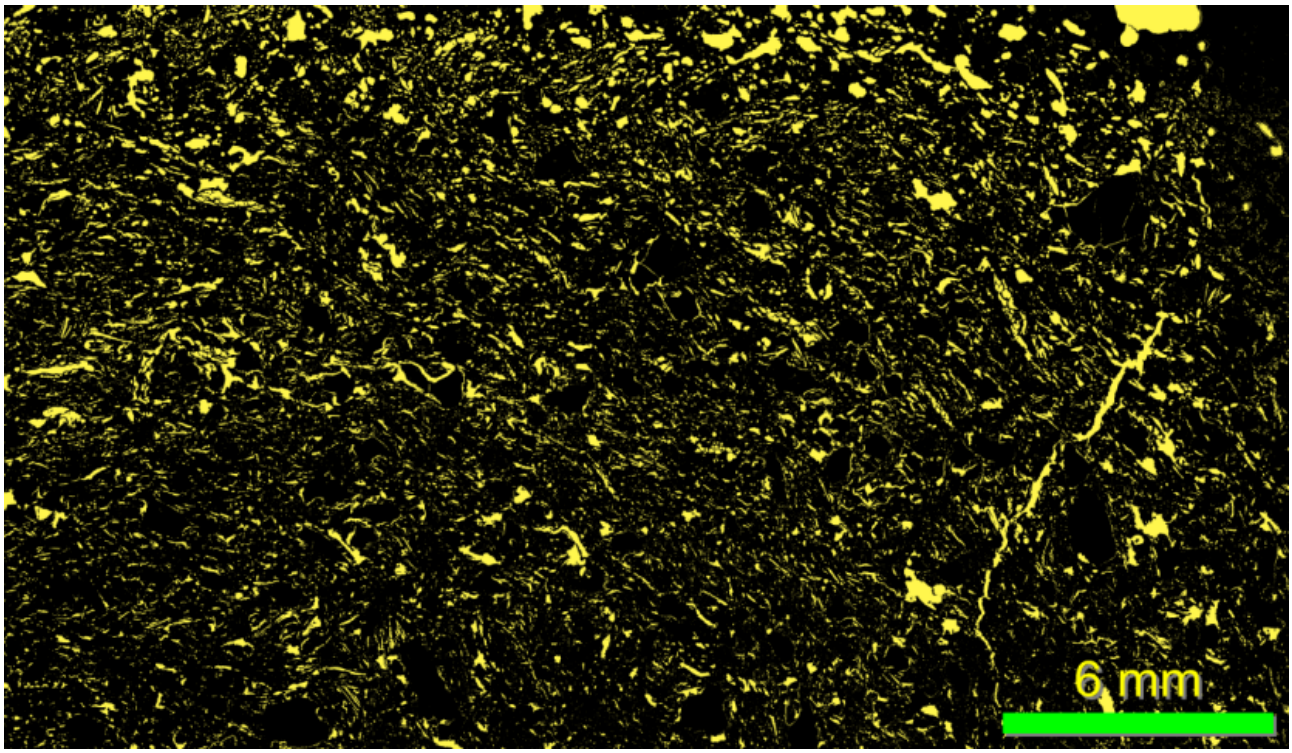

Figure 5. Historic brick (from the Read House in New Castle, Delaware) with a very stringy network of many (over 6,500) small pores.

Finally, once a pore network has been correctly segmented, we can collect data on many parameters in addition to area percentage. Ones that have been found most useful include those related to pore size and shape. Pore size is defined by either maximum length (feret diameter) or pore area [6, 10, 39]; or by number or percentage of pores falling into various size categories, defined according to the type of material and the research questions. Many petrographers have also measured pore shape, usually determined by measuring aspect ratio and roundness. Aspect

ratio (ratio between the major and minor axis) is a measure of pore elongation; ratios between 1 – 1.5 are considered equidimensional, larger ratios indicate elongation. Roundness is defined as perimeter² / 4 π a, where a is equal to pore area [12]. Roundness measures between 1.0 and 3.0 indicate a round object, those greater than 3.0 an angular one. A round object with low aspect ratio is considered circular; with high aspect ratio it is an ellipse. Non-round objects with low aspect ratio are square; with a high one, rectangular.

As an example, we can compare the historic brick specimen in Figure 5 (from the Read House, New Castle, Delaware) with a specimen from another brick found at a different location within the same site (Figure 6). Table 3 compares the data for the two bricks, including Total Optical Porosity, size (length/ferret diameter), aspect ratio, and roundness, and shows that there are some significant differences between the bricks. While both have the same Total Optical Porosity, the brick in Figure 6 has a much higher amount of that accounted for by large pores, fewer in number than the brick in Figure 5 (under 1,000 versus over 6,500).The pores of the brick in Figure 5 are often smaller, significantly more elongated (higher aspect ratio), and more angular. Removing from analysis pores that touch borders had little effect on the results, indicating that this issue is not as significant when an entire thin section is analyzed compared with its effect on microscopic fields of view. The results of this example from the Read House bricks indicate that different construction campaigns used bricks from different sources. This hypothesis is supported by a more extensive case study.

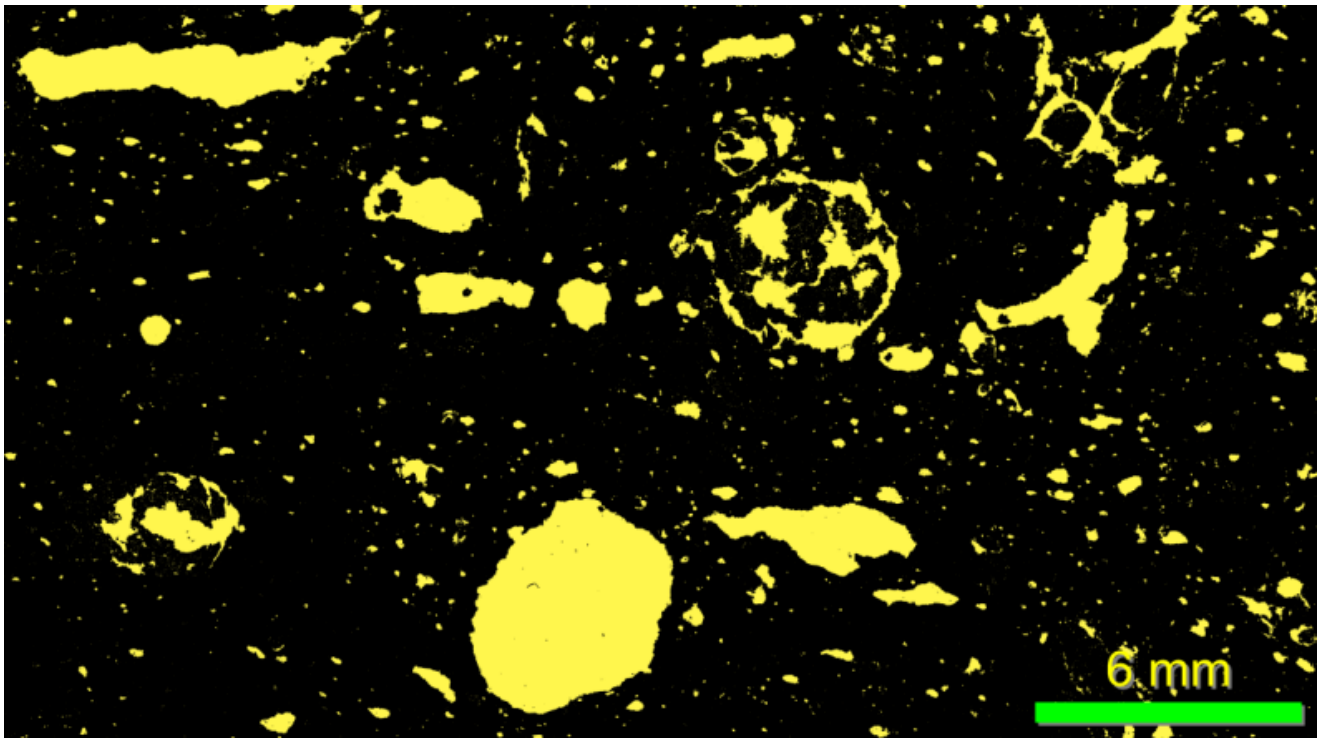

Figure 6. Historic brick (from Read House, New Castle, Delaware) excavated from a different area of the site than the brick in Figure 5. Total Optical Porosity of the bricks are identical, but a much higher amount of the porosity here is accounted for by large pores that are significantly less elongated (lower aspect ratio) and much more round.

Table 3. Porosity Characteristics of Bricks Excavated From Different Locations at Read House, New Castle, DE

	Brick 1	**Brick 2**
Total Optical Porosity (%)		
Pores ≥ 0.007 mm	14	14
Pores ≥ 0.063 mm	12	13
Pores ≥ 0.2 mm	7.6	13
Pores ≥ 0.63 mm	2.2	11
Length (feret diameter) (mm)		
Pores ≥ 0.007 mm, maximum	3.5	7.8
Pores ≥ 0.007 mm, mean	0.07	0.11
Pores ≥ 0.063 mm, mean	0.15	0.24
Pores ≥ 0.2 mm, mean	0.34	0.58
Pores ≥ 0.63 mm, mean	1.0	1.8
Aspect Ratio, mean		
Pores ≥ 0.007 mm	2.4	2.1
Pores ≥ 0.063 mm	3.1	2.1
Pores ≥ 0.2 mm	3.8	2.2
Pores ≥ 0.63 mm	4.0	2.6
Roundness, mean		
Pores ≥ 0.007 mm	2.4	2.1
Pores ≥ 0.063 mm	3.5	2.3
Pores ≥ 0.2 mm	4.8	3.0
Pores ≥ 0.63 mm	9.3	5.7
Perimeter, mean (mm)		
Pores ≥ 0.007 mm	0.18	0.34
Pores ≥ 0.063 mm	0.41	0.79
Pores ≥ 0.2 mm	1.0	2.1
Pores ≥ 0.63 mm	3.7	7.0
Area, mean (mm^2)		
Pores ≥ 0.007 mm	<0.01	0.03
Pores ≥ 0.063 mm	0.01	0.08
Pores ≥ 0.2 mm	0.03	0.27
Pores ≥ 0.63 mm	0.17	1.3
Sand (% ≥ 0.063 mm)	20	10

Analysis using Smart Segmentation (Image-Pro Premier); 0.063 mm is lower limit for fine sand, 0.2 for medium sand, and 0.63 for coarse sand [17] so were used for pore size categorization.

CONCLUSIONS

These experiments with laboratory-prepared specimens made with two different clays of very different visual appearances and with sand additions of varying sizes and amounts have

demonstrated that digital image analysis of petrographic thin sections can be a fast, reliable, and reproducible method for quantifying macropore systems in ceramic materials. Key elements of the successful procedure include using a thin section impregnated with a dyed epoxy to highlight pores, use of a high-resolution scan of an entire thin section, and development of a carefully-constructed segmentation recipe that can be applied to all thin sections of a similar appearance. Total Optical Porosity and data quantifying the pore sizes and shapes can be used to characterize a ceramic product or ware and to compare it with others. While fully interpreting the reasons for the amount, shape, and size distribution of pores and pore networks in ancient and historic ceramics may be very complex and difficult, characterization of visible pores can provide a "porosity fingerprint" for a material [12]. Such porosity fingerprints may help in identifying similar materials, grouping materials, or, in conjunction with other petrographic and chemical data, in identifying workshops. Application of the methods discussed here to historic and archaeological case studies, such as the Read House bricks, are now helping us to better interpret and understand choices that workshops made in materials selection, processing, fabrication, and firing procedures, and how those choices affected the final ceramic products made and used by past societies.

ACKNOWLEDGMENTS

This work was supported by the National Science Foundation under Grant No. 1005992. Yimeng Liu in the University of Delaware's Center for Historic Architecture and Design helped with the fabrication and firing of the experimental specimens, and Dr. Lu Ann DeCunzo (University of Delaware Anthropology Department) provided the Read House brick specimens.

REFERENCES

1. P. Rice, *Pottery Analysis: A Sourcebook* (University of Chicago Press, Chicago, 1987).
2. C. L. Reedy, *Thin-section Petrography of Stone and Ceramic Cultural Materials* (Archetype Publications, London, 2008).
3. P. S. Quinn (editor), *Interpreting Silent Artefacts: Petrographic Approaches to Archaeological Materials (*Archaeopress, Oxford, 2009).
4. P. S. Quinn, *Ceramic Petrography: The Interpretation of Archaeological Pottery & Related Artefacts in Thin Section* (Archaeopress, Oxford, 2013).
5. O. S. Rye, Archaeology & Physical Anthropology in Oceania **11** (2), 106-137 (1976).
6. G. Cultrone, E. Sebastián, K. Elert, M. J. de la Toree, O. Cazalla, and C. Rodriguez-Navarro, Journal of the European Ceramic Society **24**, 547-564 (2004).
7. C. K. Koh Choo, Y. E. Lee, I. W. Shim, W. K. Choo, G. H. Kim, W. Y. Hug, and S. Chun, Archaeometry **46** (2), 247-265 (2004).
8. K. G. Harry and A. Johnson, Journal of Archaeological Sciences **31**, 1567-1575 (2004).
9. D. Miriello and G. M. Crisci, Journal of Cultural Heritage **7**, 186-192 (2006).
10. U. Mueller and E. F. Hansen, in *Proceedings of the 8th Euroseminar on Microscopy Applied to Building Materials*, edited by B. Georgalia and E. E. Toumbakari, (Cosmosware, Athens, 2001), pp. 603-610.
11. S. Deshpande, A. Kulkarni, S. Sampath, and H. Herman, Surface Coatings & Technology **187**, 6-16 (2004).
12. J. M. Layman, MS. Thesis, Texas A & M University, 2002.

13. IUPAC, Pure Applied Chemistry **31**, 578-638 (1972).
14. E. Borrelli, *Porosity* (ICCROM, Rome, 1999).
15. F. Anselmetti, S. Luthi, and G. P., Eberli, American Association of Petroleum Geologists Bulletin **82** (10), 1815-1836 (1998).
16. N. S. I. Bashah and B. Pierson, in *Quantification of Pore Structure in a Miocene Carbonate Build-up of Central Luconia, Sarawak and its Relationship to Sonic Velocity* (International Petroleum Technology Conference, Bangkok), DOI 0.1523/14625.MS.
17. D. Norbury, *Soil and Rock Description in Engineering Practice* (CRC Press, Boca Raton, 2010).
18. M. Pagliari, N. Vignozzi, and S. Pellegrini, Soil & Tillage Research **79**, 131-143 (2004).
19. M. von Bradke, M. F. Gritzhofer, and R. Henne, Scanning **27**, 132-135 (2005).
20. A. Adams, PhD. Thesis, Texas A & M University, 2005.
21. T. T. Mowers and D. A. Budd, American Association of Petroleum Geologists Bulletin **80,** 309-322 (1996).
22. E. Moreau, B. Velde, and F. Terribile, Geoderma **92**, 55-72 (1999).
23. V. Marcelino, V. Cnudde, V. Vansteelandt, and F. Caro, European Journal of Soil Science **58**, 133-140 (2007).
24. A. Schmitt, Archaeometry **40** (2), 293-310 (1998).
25. C. L. Reedy, Journal of the American Institute for Conservation **45** (2), 127-146 (2006).
26. R. Erlich, S. K. Kennedy, S. J. Crabtree, and R. L. Cannon, Journal of Sedimentary Petrology **54**, 1365-1378 (1984).
27. A. Nijboer, P. Attema, and G. Van Oortmerssen, Paleohistoria **47/48**, 141-205 (2006).
28. G. A. Thompson and D. A. Jerram, presented at the 2003 British Sedimentological Research Group General Meeting, Leeds, England (unpublished).
29. T. L. De Keyser, Journal of Sedimentary Research **69** (4), 962-964 (1999).
30. E. F. Hansen, PhD. Thesis, University of California, Los Angeles, 2000.
31. S. Tarquini and P. Armienti, Image Analysis and Stereology **22**, 27-34 (2003).
32. F. Casadio, G. Chiari, and S. Simon, Archaeometry **47** (4), 671-689 (2005).
33. P. C. Livingood, in *Plaquemine Archaeology*, edited by M. A. Rees and P. C. Livingood (University of Alabama Press, Tuscaloosa, 2007), pp. 108-126.
34. E. Frahm, M. Nikolaidou, and M. Kelly-Buccelati, SAS Bulletin **32** (2), 8-12 (2008).
35. E. H. Van Den Berg, V. F. Bense, and W. Schlager, Journal of Sedimentary Research **73** (1), 133-143 (2003).
36. J. Carlson, L. Sutter, T. Van Dam, and K. W. Peterson, Transportation Research Record (Concrete Materials) **1979**, 54-59 (2006).
37. S. Tarquini and M. Favalli, Computers & Geosciences **36**, 665-74 (2010).
38. C. L. Reedy, Studies in Conservation **57** (S1), 227-233 (2012).
39. C. M. Dicus, MS Thesis, Texas A & M University, 2007.